PCCP

Accepted Manuscript

This is an *Accepted Manuscript*, which has been through the Royal Society of Chemistry peer review process and has been accepted for publication.

Accepted Manuscripts are published online shortly after acceptance, before technical editing, formatting and proof reading. Using this free service, authors can make their results available to the community, in citable form, before we publish the edited article. We will replace this *Accepted Manuscript* with the edited and formatted *Advance Article* as soon as it is available.

You can find more information about *Accepted Manuscripts* in the **Information for Authors**.

Please note that technical editing may introduce minor changes to the text and/or graphics, which may alter content. The journal's standard **Terms & Conditions** and the **Ethical guidelines** still apply. In no event shall the Royal Society of Chemistry be held responsible for any errors or omissions in this *Accepted Manuscript* or any consequences arising from the use of any information it contains.

Journal Name

Dielectric relaxations of polyether-based polyurethanes containing ionic liquids as antistatic agents

Akiko Tsurumaki,[a,b,c] Federico Bertasi,[d] Keti Vezzù,[d] Enrico Negro,[d] Vito Di Noto,[d,e] and Hiroyuki Ohno[a,b,c,*]

Dielectric properties of polyurethanes containing poly(propylene oxide) (PO) and poly(ethylene oxide) (EO) units are discussed with results of direct current (DC) measurements and broadband electrical spectroscopy (BES) studies. Dielectric properties of polyether-containing polyurethanes (PUs) are compared to those of PUs containing 1000 ppm of ionic liquids (ILs) as antistatic agents. The effect of the chemical environment of these ILs such as in anion-fixed polymers (PU-AF), cation-fixed polymers (PU-CF), and where the IL was simply mixed with the PUs (PU-IL) is compared and discussed on the basis of ion mobility. DC measurements suggest that the charge current is attributed not only to the electrode polarization but also to continuous dielectric relaxation. BES studies elucidate that both fast and slow relaxations are taking place in EO-rich domains in pristine PU and PU-AF. The activation energies of the slow relaxation and of the ionic conductivity are similar, suggesting that the ionic conductivity of these materials is attributed to the ion exchange reaction in EO/ion complexes. In contrast, only fast relaxations are observed in the domains mostly comprised by ion-depleted EO in the PUs containing "free" anions, i.e., PU-CF and PU-IL. This suggests that [Tf$_2$N]$^-$ are weakly interacting with the EO chains and contribute effectively to the ion conduction. Thus, an enhanced ionic conductivity is observed in PU-CF and PU-IL, yielding a sufficient antistatic effect. Taking into account its long shelf life arising from no fear of IL bleed-out, PU-CF is concluded to be the most promising candidate.

1. Introduction

Ionic liquids (ILs) have been recognized as potential additives for polymers for plasticising the materials.[1] In the area of solid-state polymer electrolytes, the composites based on polyethers such as poly(ethylene oxide) (PEO) and ILs have long been investigated as ion-conducting materials.[2] Improved ionic conductivity is attributed to the plasticising effect, in other words, low glass transition temperature (T_g) of ILs. This also provides higher concentration of free and mobile ions.

Polyurethanes have been expected to be widely applicable materials in industry. The properties of polyurethanes can be controlled variedly by not only using additives but also changing a combination of precursors; i.e., polyols and polyisocyanates.[3] The latter methodology inhibits hazardous pollution which is triggered by the bleed out of the additives.

Another important advantage of polyurethanes is balanced properties of rubber-like elasticity and plastic-like toughness. Flexible polyurethanes can be obtained with polyether-based polyols; these are known to show an excellent flexibility.[4] Polyether-based polyurethanes (PUs, hereafter) are expected to be used in form of sheet, film, and membrane for production of precision devices. However, as well as other polymers, the PUs are insulators and cause serious damage in the precision devices through electrostatic discharges.

To solve this problem, several different antistatic agents have been examined. Surfactants show a positive effect because of the enhanced ionic conductivity originated by the adsorbed moisture on the polymer surface.[5] Due to this conduction mechanism, they enhance the effect only under humid conditions; however, the adsorbed water is easily wiped out. On the other hand, carbon black and inorganic fillers give rise to an antistatic effect by the electron conduction through the successive conduction path of the fillers.[6] The addition of these fillers to form successive conduction path deteriorates properties of host polymers such as transparency and mechanical stability. Accordingly, there is a strong requirement to design additives which: 1) enhance the antistatic effect in small amounts of addition; and 2) are sustainably effective under various conditions.

Taking the great contribution of ILs to ionic conductivity in polyether matrices into account, ILs were applied as antistatic agents for the PUs.[7] It was shown that the resistivity of PU

^{a} Global Innovation Research Organization, Tokyo University of Agriculture and Technology, 2-24-16 Naka-cho, Koganei, Tokyo 184-8588, Japan.
^{b} Department of Biotechnology, Tokyo University of Agriculture and Technology, 2-24-16 Naka-cho, Koganei, Tokyo 184-8588, Japan.
^{c} Functional Ionic Liquid Laboratories, Graduate School of Engineering, Tokyo University of Agriculture and Technology,Japan.
^{d} Department of Chemical Sciences, University of Padova, Via Marzolo 1, 35131 Padova (PD), Italy.
^{e} Department of Industrial Engineering, University of Padova, Via Gradenigo, 6/a - 35131 Padova (PD), Italy.
† Electronic Supplementary Information (ESI) available: See DOI: 10. 1039/x0xx00000x

films was reduced from 2.1×10^{12} to 5.5×10^{9} ohm cm^{-2} under dry conditions upon addition of only 500 ppm of 1-butyl-3-methylimidazolium bis(trifluoromethanesulfonyl)imide ([C$_4$mim][Tf$_2$N]). Furthermore, their antistatic effect was retainable after methanol rinsing of the PU films. Similar antistatic effects were observed for other [Tf$_2$N] salts. In contrast, antistatic effect changed depending on the anion structure.[8] The choice of anion structure is a key to design suitable antistatic agents for the PUs. In order to improve the credibility of antistatic effects, ILs were fixed onto the PUs *via* urethane bonds.[9] When anions were fixed onto the PUs, the films showed a poor antistatic effect even if the ILs exhibited an antistatic effect in PEO films. On the other hand, cation-fixed PU films showed comparable antistatic effect to IL-doped PUs even if the cations were fixed onto the PUs. In this study, the dielectric properties of the PUs containing ILs have been discussed to elucidate the contributions arising from the presence of free anions.

2. Experimental section

2.1. Materials

Fig. 1 shows structure of ILs and polyether-based PUs used in this study. Glycolic acid (H[Glyco], >98.0 %, from Tokyo Chemical Industry Co., Ltd.), tris(2-hydroxyethyl)methyl-ammonium CH$_3$SO$_4$ ([thema]CH$_3$SO$_4$, ≥95 %, from Sigma Aldrich Co. LLC.), bis(trifluoromethanesulfonyl)imide (H[Tf$_2$N], 70 % aqueous solution, from Rhodia), *N,N*-diethyl-*N*-methyl-*N*-(2-methoxyethyl)ammonium [Tf$_2$N] ([DEME][Tf$_2$N], ≥99 %, from Kanto Chemical Co.), and trimethylpropylammonium [Tf$_2$N] ([N$_{1113}$][Tf$_2$N], ≥97 %, from Kanto Chemical Co.) were purchased and used as received. Precursors for the PU such as polymeric diphenylmethylenediisocyanate, Sumidur 44V20 (PDI, from Sumika Bayer Urethane Chemical Co., Ltd.), trifunctional polyether polyols based on propylene-ethylene oxides 80/20 by mol/mol (P(PO/EO), Mw = 7,000, from Asahi Glass Co., Ltd.), and dibutyltin dilaurate (DBTDL, from Kyodo Yakuhin Co., Ltd.) were purchased and used without further purification. DBTDL was diluted tenfold with of Exxsol™ D40 Fluid (from ExxonMobil Chemical).

2.2. Synthesis of ILs

[thema][Tf$_2$N]: First, [thema]CH$_3$SO$_4$ was diluted ten-fold with Milli-Q water, and passed through a column filled with an anion exchange resin (Amberlite IRN-78) to give an aqueous solution of [thema]OH. To the resulting solution, an equimolar amount of aqueous H[Tf$_2$N] solution was added dropwise; the obtained neutralised solution was concentrated by evaporation. The crude product was dissolved in acetone and then passed through a short column filled with activated aluminium oxide. Acetone was removed by evaporation and the resulting liquid was dried under vacuum at 60 °C for at least 3 h. The target product was obtained as a colorless liquid. ^{1}H-NMR (400MHz, DMSO-*d*$_6$, *δ*/ppm relative to Me$_4$Si): 3.14 (3H, s, NC*H*$_3$), 3.52 (6H, t, *J* = 4.0 Hz, NC*H*$_2$CH$_2$), 3.84 (6H, m, CH$_2$C*H*$_2$OH), 5.24 (3H, t, *J* = 4.0 Hz, O*H*).

[DEME][Glyco]: This IL was prepared by the same procedure as described above for [thema][Tf$_2$N] with the corresponding [DEME] salt and acid; [DEME][Tf$_2$N] and H[Glyco]. ^{1}H-NMR (400MHz, CDCl$_3$, *δ*/ppm relative to Me$_4$Si): 1. 38 (6H, t, *J* = 7.2 Hz, C*H$_3$*CH$_2$NCH$_2$C*H$_3$*), 3.20 (3H, s, NC*H$_3$*), 3.38 (3H, s, OC*H$_3$*), 3.57 (4H, q, *J* = 9.2 Hz, CH$_3$C*H$_2$*NC*H$_2$*CH$_3$), 3.76 (2H, t, *J* = 4.4 Hz, NC*H$_2$*CH$_2$OCH$_3$), 3.83 (2H, s, C*H$_2$*COO), 3.91 (2H, s, C*H$_2$*OCH$_3$), 6.52 (1H, s, broad, O*H*).

2.3. Film preparation

The PU films were prepared with 50.0 g of P(PO/EO), 3.59 g of PDI, and 0.9 g of DBTDL solution as a catalyst. This mixture was further mixed homogeneously by MAZERUSTAR KK-102 (from Kurabo Industries Ltd.), then cast on a glass plate with a 0.1 mm spacer. The plate was heated to 80 °C for 30 min, and the PUs were obtained as a thin film (thickness = 0.1 ± 0.05 mm). PUs containing 1000 ppm of the ILs were prepared by the same procedure as the pure PU films by using P(PO/EO)-dried IL mixtures instead of pure P(PO/EO). Since hydroxyl groups are known to form urethane bonds with the isocyanate, ILs composed of either cations (*i.e.*, [thema][Tf$_2$N]) or anions (*i.e.*, [DEME][Glyco]) comprising hydroxyl groups were used to prepare cation-fixed PUs (PU-CF) and anion-fixed PUs (PU-AF), respectively. Similarly, the IL containing no hydroxyl groups (*i.e.*, [N$_{1113}$][Tf$_2$N]) was used to prepare a simple mixture of IL and PUs, indicated as IL-doped PUs (PU-IL). All films were dried at 60 °C for at least 3 h before measurements

2.4. Direct current (DC) measurements

DC was measured with a Modulab system (from Solartron) at room temperature. Cells printed with comb-shaped gold electrodes with a four-pair-toothed formation were used for the DC measurement. A squarely cut film was sandwiched with the cell and a glass plate, and was tightly packed under N$_2$ atmosphere. Measurements were carried out under ambient atmosphere. Prior to the measurements, a potential of −5.0 V was applied for 60 sec to generate the same static environment on the film surfaces; afterwards, DC was successively measured by alternatively applying +5.0 V and 0 V for 1000 sec.
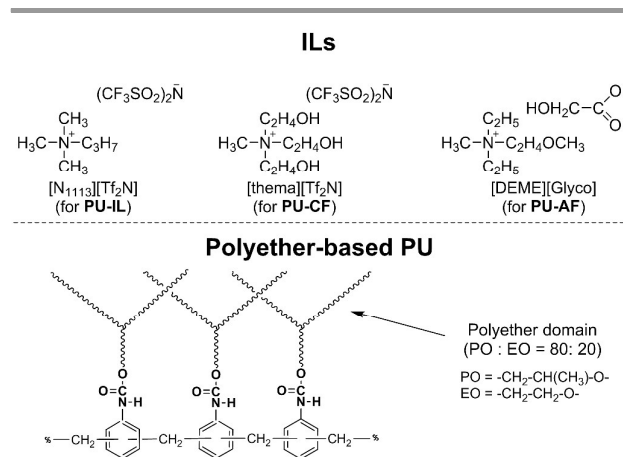
Fig. 1. Structure of ILs and polyether-based PUs used in this study.

2.5. Modulated differential scanning calorimetry(MDSC)

MDSC measurements were carried out with a MDSC 2920 system (from TA Instruments) equipped with the LNCA low-temperature attachment. The sample pans were sealed in an argon filled glove box, and measurements were carried out under ambient atmosphere. MDSC scans were taken in a temperature range from -120 to +150 °C with a scan rate of 3 °C min⁻¹ on about 4 mg of the dried samples.

2.6. Broadband electrical spectroscopy (BES)

BES of polymer samples was carried out by sandwiching the film between two circular platinum electrodes with a diameter of 13 mm. The sample cells were sealed in an argon filled glove box. An Alpha A module (from Novocontrol) equipped with an home-made temperature controller was used to measure spectra in a temperature range from -80 to +100 °C in increasing steps of 10 °C. The temperature was set with an error of ±0.2 °C. The frequencies have been scanned from 0.03 Hz to 10 MHz.

3. Results and discussion

Fig. 2 shows the time dependence of current change when 5.0 and 0.0 V were applied to the PU-films. In order to postulate that the anion was the only conductive ion species, PU-CF (cation-fixed system) containing 1000 ppm of [thema][Tf$_2$N] was used, and its current decay was compared to that of the pure PUs. Initial charge currents (I_c(t), t = 1) of 0.0075 and 3.6 nA cm^{-2} were measured for PU and PU-CF, respectively. A surface resistivity was equal to the reciprocal of this initial charge current. The desired resistivity (< 10^{10} ohm cm^{-2}) was measured for PU-CF. These charge currents gradually decrease as the duration of measurement increase; they converge to 0.0046 and 0.23 nA cm^{-2}, frequently recognized as the leakage current (I_∞(t)). The I_c(t) measurement is correlated to the rates of dynamical phenomena characterising the electric response of investigated materials. Therefore, there are good correlation between I_c(t) curves in the time domain (Fig. 2) and I(t) calculated from the results of BES measurement (see Fig.

S1 in the supplementary Information). I(t) was obtained by taking the inverse Fourier transform of the r.t. complex permittivity ($\varepsilon^*(\omega)$) spectra.[10] The r.t. $\varepsilon^*(\omega)$ spectra were discussed in details below. Similar trend of I_c(t) and I(t) proves that time-domain conductimetry and the frequency–domain electrical spectroscopy are complementary techniques, which provide consistent results, and which allow to fully clarify the mechanisms of action of investigated materials. Comparison of I_c(t) and I(t) allows to reveal that a fast fluctuation (> 1 Hz) influence the I_c(t) behaviour at very short time, while the polarization phenomenon is mostly affecting the I_c(t) values in their medium time regime (see Fig. 2 and Fig. S1).

When these samples were kept at 0.0 V, the discharge current (I_d(t)) was observed. For the case of glassy state materials, the current change obeys Eq. 1 when the conductivity is enhanced through the relaxation of the materials and Ohm's law is valid at any moment of measurement.[11]

$$-I_d(t) = I_c(t-t_1) - I_\infty(t_1) \quad \textbf{(Eq. 1)}$$

Where t$_1$ is the time when the steady voltage is removed (in this study, 1000 sec where the current reached almost a constant value). This equation is based on the superposition principle. Glassy materials follow this principle below their T_g and deviate as the temperature increased. The deviation arises from the space charge polarization (*i.e.*, electrode polarization) of the material. When t = 1001, R.H.S. is found to be 0.0029 nA cm^{-2} and L.H.S is 0.0028 nA cm^{-2} for the pristine PU film. On the other hand, R.H.S. is 3.37 nA cm^{-2} and L.H.S is found to be 0.48 nA cm^{-2} for PU-CF. The quite small -I_d(t) compared to I_c(t-t$_1$) - I_∞(t$_1$) suggests that charge currents are enhanced not only by dielectric relaxations but mostly by electrode polarization. Then, we calculated the amount of anions in PU-CF to discuss whether there exist enough charged species to enhance the initial direct current. For the case of PU films containing 1000 ppm of [thema][Tf$_2$N], there exist about 1.8 × 10^{16} of [Tf$_2$N]$^-$ in the square film. The quantity of charge Q_t of the film is calculated from Eq. 2.

$$Q_t = \int_0^t I_c(t)dt \quad \textbf{(Eq. 2)}$$
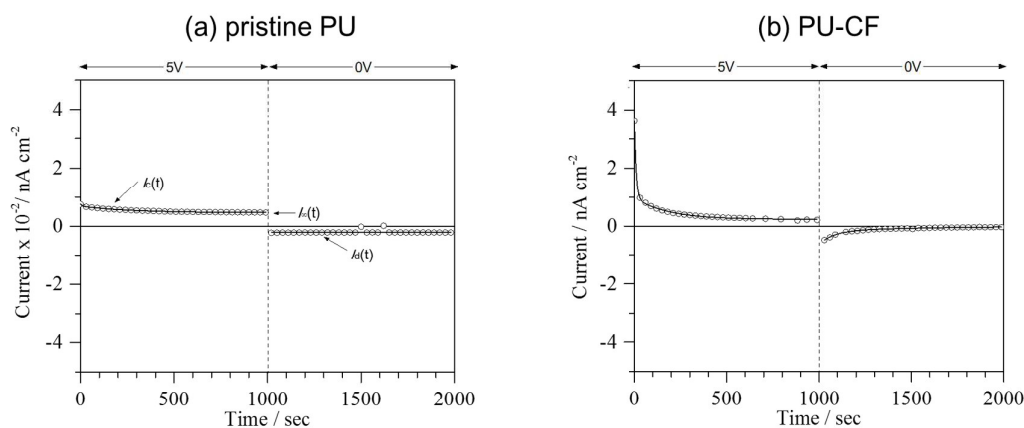
Fig. 2. Current decay charged at 5.0 V and discharge current observed under 0 V.

ARTICLE

Journal Name

(a), (c) pristine PU

(b), (d) PU-CF
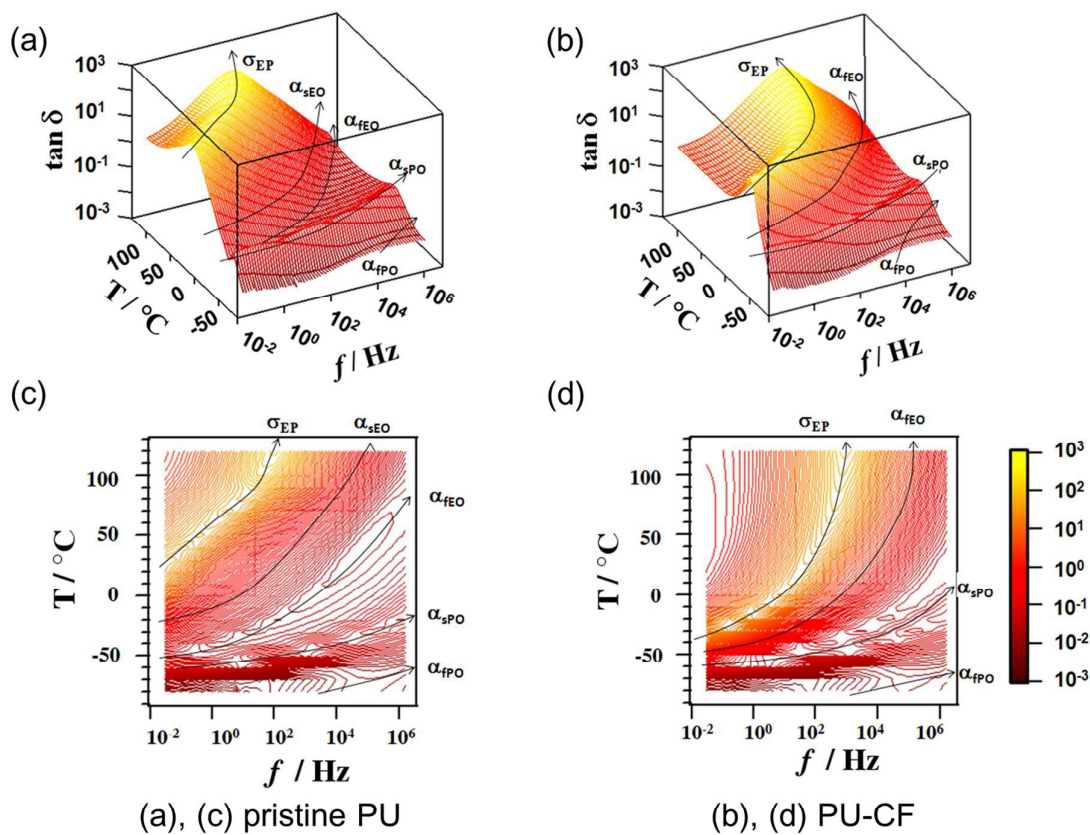
Fig. 3. Tanδ *vs.* temperature and frequency in 3D (a, b) and contour map (c, d).
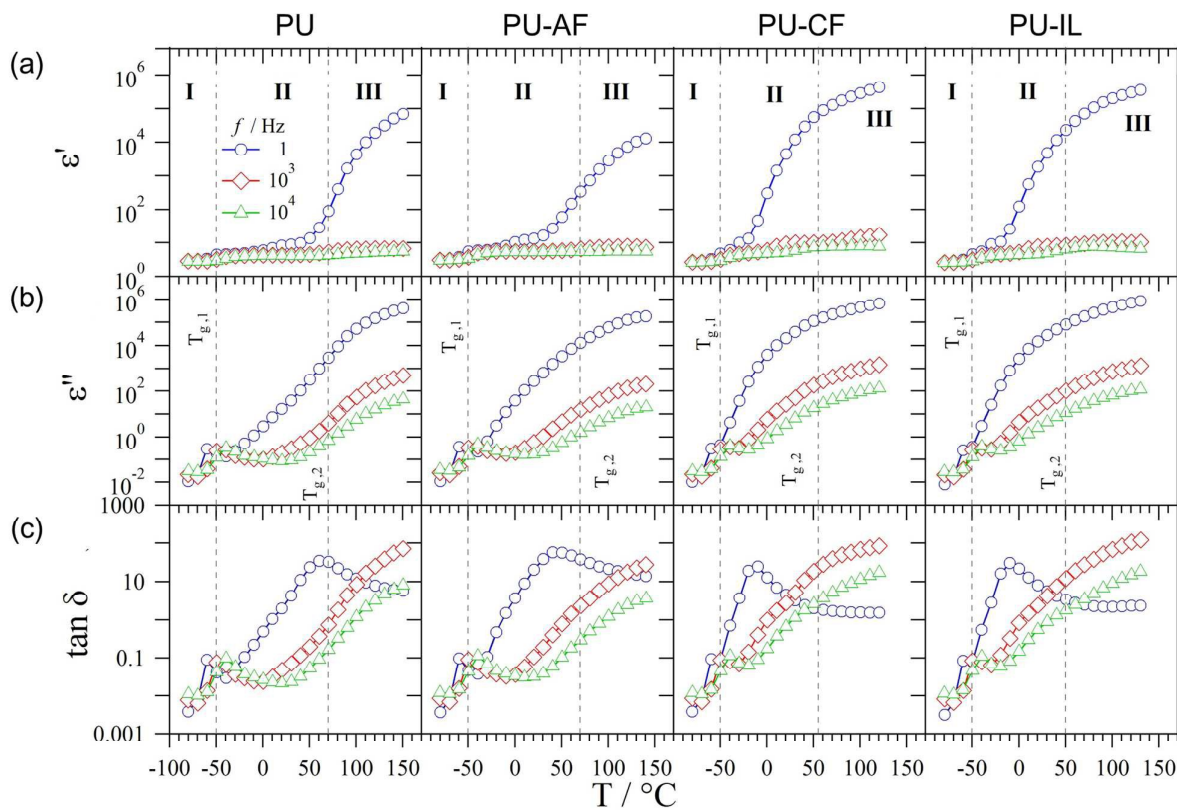
Fig. 4. (a) ε', (b) ε'' and (c) tanδ *vs.* temperature at 1, 10^3 and 10^4 Hz (circle, rhombus, and triangle).

When we consider the initial $I_c(t)$, Q_1 is calculated to be 3.6 × 10^{-9} C cm^{-2}. Considering the elementary charge (e = 1. 602 × 10^{-19} C), Q_1 is found to be equivalent to a total charge for 2.2 × 10^{10} of the charged species. This number is small enough as compared with the number of [Tf$_2$N]$^-$ in PU-CF. On the other hand, when Q_t is calculated for t from 0 to 1000 sec, Q_{1000} is found to be 3.9 × 10^{-7} C cm^{-2}, which is equivalent to a total charge for 2.4 × 10^{12} of charged species. Taking the diffusion coefficient into account, the amount of [Tf$_2$N]$^-$ in the investigated film is not enough to enhance initial $I_c(t)$ and retain $I_\infty(t)$. All results of DC measurement suggest that $I_c(t)$, especially $I_\infty(t)$, is modulated by the electrode polarization event of ILs. Then, BES measurements were carried out to clarify the electrical response in terms of conductivity and permittivity of pristine PU, PU-AF, PU-CF, and PU-IL.

Tan δ vs. temperature and frequency for pristine PU and PU-CF are shown in Fig. 3, and that for PU-AF and PU-IL are shown in the Supplementary Information (Fig. S2). Electrode polarization phenomena (EPs) which are associated to the accumulation of charge at the interface between the electrode and the sample are observed in all the samples. This phenomenon depends on the mobility of the charge towards the electrode surface, thus this polarization is detected at low frequencies. EPs are shifted to higher frequencies as the temperature increases and as the conductivity of the samples (σ_{EP}) increases (see Fig. S3 in the Supplementary Information). The EP relaxation frequency of each sample (f_{EP}) relates to the relaxation time τ_{EP} = 1/(2πf_{EP}) with f_{EP} proportional to: (i) the Debye length (L_D); and (ii) the density and mobility of charges in the electronic double layer. Thus, f_{EP} is correlated to the accumulation of charges "free" to move at the interface

between the electrode and the materials. In detail, if we consider that: (i) L_D is constant; and (ii) with the exception of pristine PU the concentration of ions in the materials is similar, a higher f_{EP} value in PU-CF and PU-IL reveals that in these systems the charge mobility is higher than that of pristine PU and PU-AF. On this basis it is easy to conclude that, with respect to PU and PU-AF, in PU-CF and PU-IL a higher value of charge mobility is responsible of the large ε' intensity values in the profiles of the electrode polarization events. The details of the difference in ε are also shown in Fig. 4(a). At T > 20 °C, the steep rise of ε' profiles was observed at 1.0 Hz, which corresponded to the electrode polarization phenomenon. A larger ε' was observed for PU-CF and PU-IL, while the opposite trend was detected for PU-AF with respect to pristine PU. These results suggest that the PU-based samples with "free" anions present high charge mobility and an increased polarizability effect, which raises the conductivity and therefore enhances the excellent antistatic properties of these materials.

The MDSC profiles of Fig. 5 suggest two T_gs. The most intense glass transition $T_{g,1}$ is detected at ca. -62 °C, while the weak $T_{g,2}$ is observed at ca. +55 °C. A careful analysis of the stoichiometry reveals that in the pristine PU the urethane/EO/PO ratio is 1:6.7:26.5. This indicates that in pristine PU, EO and PO repeat units are predominating. In the soft domains, EO and PO respectively comprise 20 % and 80 %. These results suggest that on average the soft random polymer block is mainly formed by two domains. The former, which is the most flexible, is rich in PO repeat units and is responsible of the low-temperature $T_{g,1}$ at ca. -62 °C. The latter, which is rich in EO units, exhibits a T_g at higher temperatures ($T_{g,2}$ at around +55 °C). The influences of these thermal transition are recognizable in the spectra of the ε', ε'', and tanδ vs. temperature (Fig. 4). Indeed, the profiles measured at frequencies higher than 1 kHz show a low polarization peak at ca. -50 °C and a second transition at ca. +70 °C. Taken all together, the electric and thermal response of PU-based materials (Fig. 4) demonstrates that these systems are characterized by:

1) three regions, delimited by the $T_{g,1}$ and $T_{g,2}$ thermal transitions;
2) two dynamic glass transition events. The one detected at the lower temperature ($T_{g,1}$) is associated to the diffusion of the conformational states of the soft domain rich in PO repeat units, while that observed at the higher temperature ($T_{g,2}$) is attributed to the segmental mode of the soft domain rich in EO.

A detailed analysis of the 3D spectra of Fig. 3 and Fig. S2 (in the Supplementary Information) demonstrates that, in accordance with other studies,[12] α_{PO} and α_{EO} relaxations are both split in fast (α_{fPO} and α_{fEO}) and in slow modes (α_{sPO} and α_{sEO}). As described elsewhere,[13] traces of Na$^+$ and K$^+$ are present in polyether compounds and split their segmental modes into a slow one and a fast one. Accordingly, the polyether chains complexing the cations are more rigid, and their segmental
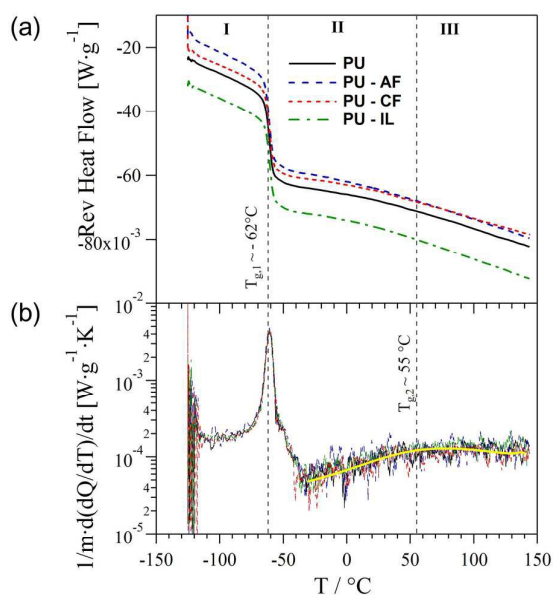
Fig. 5. The (a) MDSC and (b) MDSC derivative profiles for the pristine PU, PU-AF, PU-CF, and PU-IL samples.
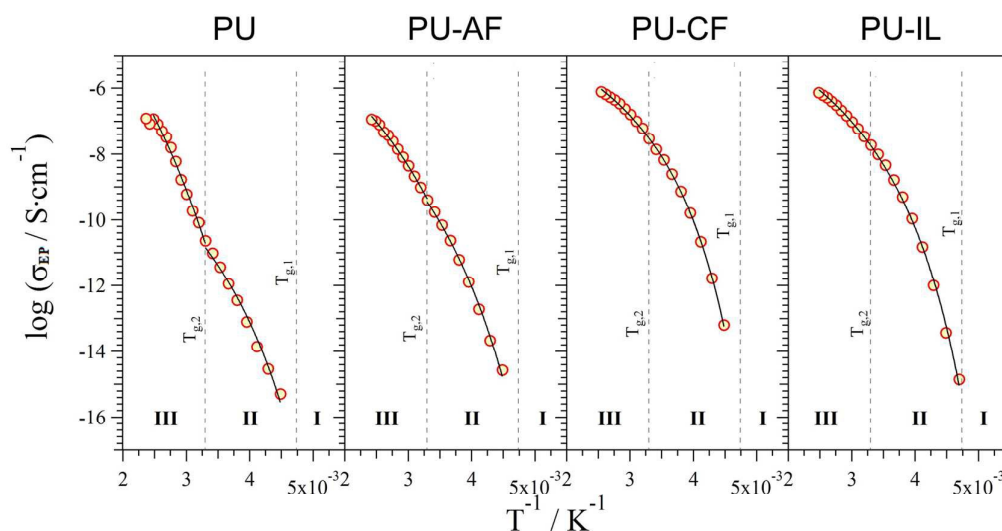
Fig. 6. Dependence of the conductivities σ_{EP} vs. $1/T$ in the investigated films. σ_{EP} is determined by fitting of the σ^*,ε^* and tanδ data (see Fig. 3, S1) with Eq. 3. The line is the fitting of σ_{EP} values by a VFT trend (see Eq. 4).

motion is slower ("slow modes"). For the ion-depleted polyether chains, "free" chains show the α relaxations detected at high frequencies (α$_{fPO}$ and α$_{fEO}$); these are the "fast modes". Therefore, α$_{sPO}$ and α$_{fPO}$ are respectively attributed to the slow and fast segmental modes of polyether domains rich in PO, while α$_{sEO}$ and α$_{fEO}$ are associated to the same modes in the soft domains rich in EO repeat units. The comparison of the 3D spectra in Fig. 3 and of tanδ in Fig. 4 clearly demonstrates that α$_{fEO}$ and α$_{sEO}$ are significantly influenced by the chemical modulation of urethane domains. Indeed, results show that:

1) in pristine PU and PU-AF both α$_{fEO}$ and α$_{sEO}$ are detected;
2) in the anion-free samples (PU-CF and PU-IL) only the α$_{fEO}$ is revealed, thus demonstrating that when a high concentration of free anions is present in urethane domains, the metal traces doping in the EO-rich domains undergo complexation, increasing the size of anion complexes [M(Tf$_2$N)$_2$]$^-$, free to move, which deplete metal traces selectively and completely from the polyether domains rich in EO repeat units.

On the other hand, α$_{fPO}$ and α$_{sPO}$ are less affected by the chemical modification of the pristine PU. This suggests that the domain rich in PO is likely:

1) located far from the urethane crosslinking domains, while EO units possibly orient to the crosslinking domains;
2) less affected by the process of ion depletion triggered by the anionic ligands.

To study in detail the phenomena underlying the measured global electric response, an accurate fitting of the data shown in Fig. 3 is carried out simultaneously in the data

representation of both the complex permittivity (ε^*), conductivity (σ^*) and tanδ profiles by means of Eq. 3.[14]

$$\varepsilon^* = \frac{\sigma_{EP}}{i\omega} \frac{(i\omega\tau_{EP})^\gamma}{[1+(i\omega\tau_{EP})^\gamma]} + \sum_i \frac{\Delta\varepsilon_i}{[1+(i\omega\tau_i)^{\alpha_i}]^{\beta_i}} + \varepsilon_\infty \quad \textbf{(Eq. 3)}$$

The first term describes the electrode polarization phenomena, where σ_{EP} is the direct current conductivity, τ_{EP} is the relaxation time of electrode polarization, ω is angular frequency, and γ is the shape parameter. The second term describes the four *i-th* detected dielectric relaxations, where $\Delta\varepsilon_i$ is the relaxation strength, τ_i is the relaxation time, α_i and β_i are the shape parameters describing respectively the symmetric and asymmetric shape of the *i-th* dielectric relaxation mode. The last term corresponds to the instantaneous permittivity, $\varepsilon_\infty = \lim_{\omega\to\infty}\varepsilon'(\omega)$.

In Fig. 6, the fitted σ_{EP} values are plotted against $1/T$. These profiles are simulated with the Vogel–Fulcher–Tamman (VFT) equation (Eq. 4):[15]

$$\sigma_{EP}(T) = \frac{A_\sigma}{\sqrt{T}}\exp\left(-\frac{E_a}{R(T-T_0)}\right) \quad \textbf{(Eq. 4)}$$

Where A_σ is related to the number of charge carriers, R is the universal gas constant, E_a is the pseudo-activation energy for conduction, and T_0 is the thermodynamic ideal glass transition temperature at which the configurational entropy becomes zero, or the "free volume" disappears. The boundary condition $(T_g - 55) \leq T_0 \leq (T_g - 40)$ is applied in order to choose the starting value for T_0.[15]

The highest σ_{EP} were measured for PU-CF and PU-IL at 25 °C followed by the σ_{EP} of PU-AF and pristine PU. The order of the σ_{EP} change agrees to that of $I_c(t)$ observed in DC measurement. It is observed that the trend of σ_{EP} vs. $1/T$ shows three conductivity regions and two VFT regions for PU and PU-AF materials, and only one VFT curve for PU-CF and PU-IL (where free [Tf$_2$N]$^-$ are present). The VFT behaviour
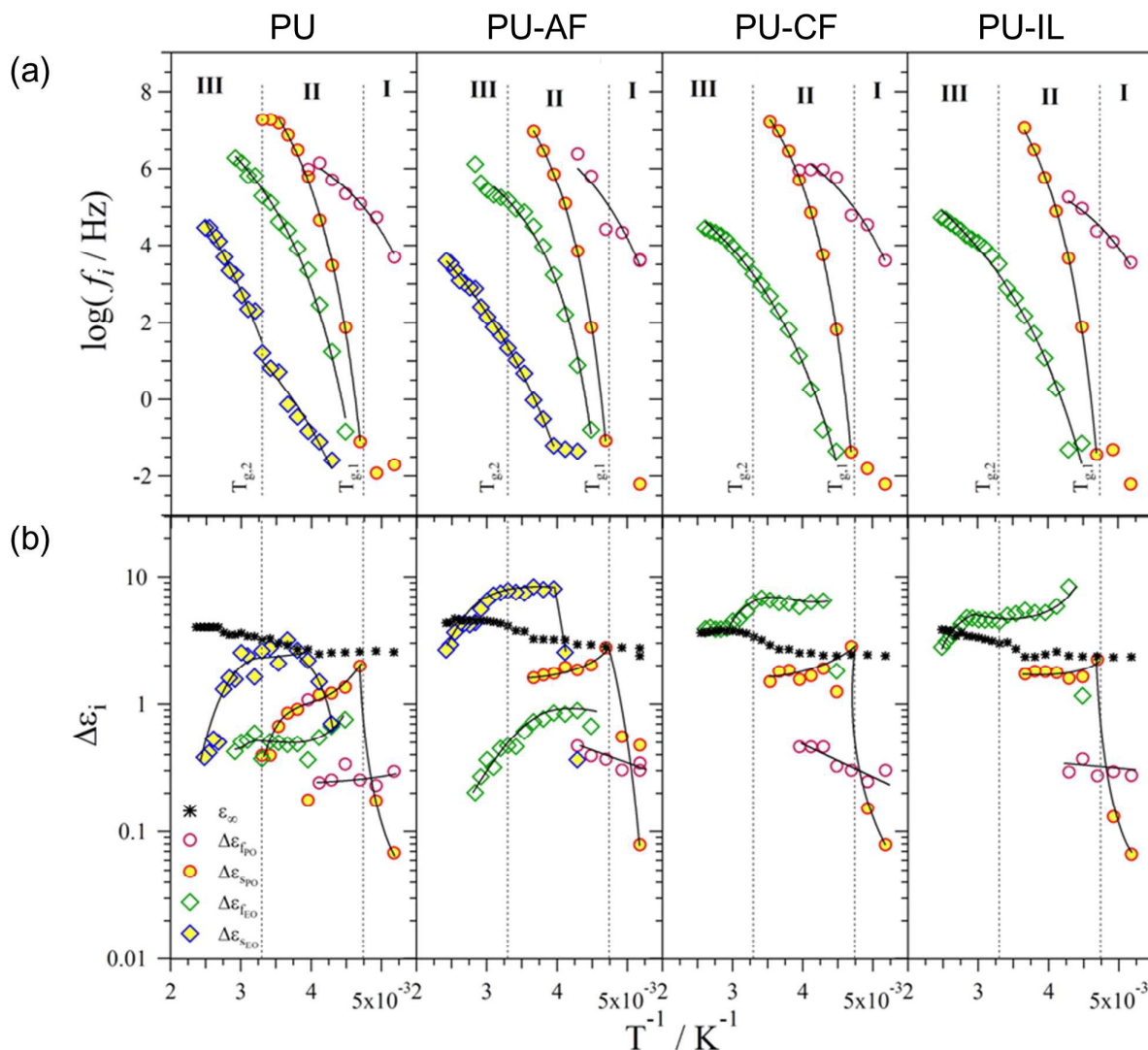
Fig. 7. Dependence on temperature of (a) f_i, and (b) $\Delta\varepsilon_i$ of i-th dielectric relaxations. Both f_i and $\Delta\varepsilon_i$ are determined by fitting ε^*, σ^* and $\tan\delta$ with Eq. 3. The profiles of f_i vs. $1/T$ are fitted by the VFTH equation (Eq. 5)

suggests that in bulk materials the migration events of charged species which are free to move are coupled with the segmental motions of the host polymer matrix (the α-modes). The low conductivity of PU-AF similar to pristine PU is attributed to the cation trapping effect of the negative charge of carboxylate oxygen chemically fixed in urethane moieties. This model accounts for the low conductivity and polarization measured in PU-AF. In the case of PU-CF and PU-IL, [Tf$_2$N]$^-$ are free to move. In details, as reported elsewhere,[16] [Tf$_2$N]$^-$ is a good ligand for alkaline or alkaline-earth metal ions to form complexes through the exchange reaction:

$$[(PO)_x \cdot (EO)_y]M^+ + 2[Tf_2N]^-$$
$$\rightarrow [(PO)_x \cdot (EO)_y] + [M(Tf_2N)_2]^-$$
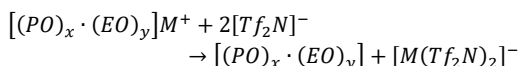
This reaction extracts the traces of alkaline and alkaline-earth metals present in EO-rich domains, eliminating the α_{sEO} mode and increasing the density in bulk materials of anion species such as [M(Tf$_2$N)$_2$]$^-$. These latter are anion complexes characterized by a larger size and a very high mobility. This phenomenon raises the conductivity of the materials endowed with "free" [Tf$_2$N]$^-$ (Fig. 6). The two VFT behaviours delimited by $T_{g,2}$ suggest that the dynamics of soft domains rich in EO repeat units play a crucial role in the modulation of long-range charge migration events.

The dielectric relaxations of the host soft polymer matrix are characterized by their own typical frequency (f_i) and dielectric strength ($\Delta\varepsilon_i$). The temperature dependence of these two parameters is shown in Fig. 7(a) and 7(b), respectively.

$$\log f_i = \log f_\infty - \frac{E_a}{R(T-T_0)} \quad \textbf{(Eq. 5)}$$

ARTICLE   Journal Name
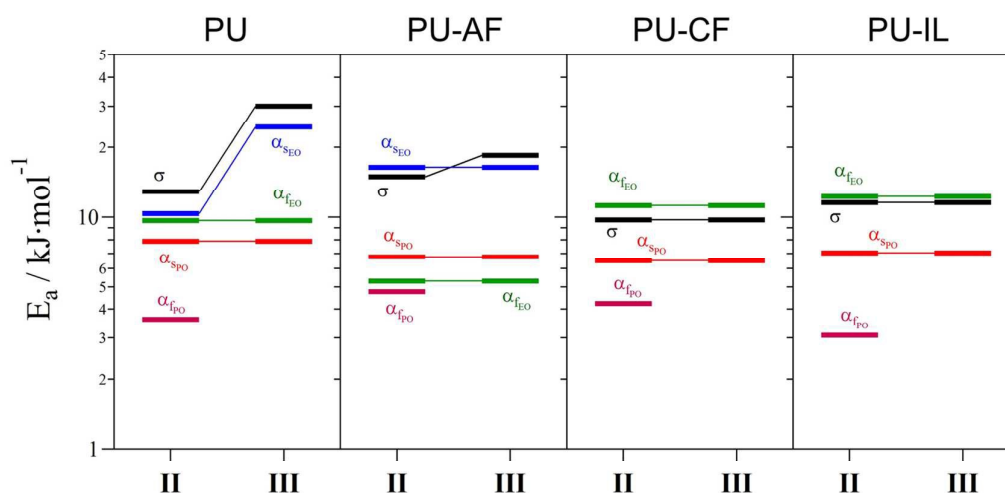
Fig. 8. Activation energies (E_a) of conduction (σ_{EP}) and of α_i modes. E_a of σ_{EP} is determined by fitting the profiles σ_{EP} *vs.* $1/T$ (Fig. 6) with the VFT equation (Eq. 4) while E_a of α_i modes is determined by fitting f_i *vs.* $1/T$ (Fig. 7(a)) with the VFTH equation (Eq. 5)

The Vogel-Fulcher-Tamman-Hesse (VFTH) dependence (Eq. 5) of the relaxation frequencies f_i and the dielectric strength $\Delta\varepsilon_i$ *vs.* temperature, are in accordance with other studies, showing α_i modes related to two types of different blocks of the co-polymer, *i.e.,* the PO- and the EO-rich domains. As previously mentioned, the molecular relaxation, α_i, detected at the highest frequencies and the lower temperatures (from -80 °C to -30 °C) is assigned to the diffusion of conformational states which takes place in the ion-depleted PO-rich domain. Other α_i are assigned to conformational fluctuation of the domain rich in PO coordinating with ion, in ion-depleted EO, and in EO with ions as temperature increase and as frequency decrease. This assignment is in perfect accordance with the two static T_gs ($T_{g,1}$ and $T_{g,2}$) detected by MDSC measurements (see Fig. 5). $\Delta\varepsilon_i$ dependence on temperature (Fig. 7(b)) shows that: 1) three regions delimited by $T_{g,1}$ at *ca.* -62 °C of PO-rich domain and $T_{g,2}$ at around +55 °C of EO-rich domain are present in the materials; and 2) the same behaviour in the intensity of α_{sPO} and α_{fPO} is observed, which confirms that the soft block rich in PO repeat units is less affected by the type of structural features which characterizes the investigated samples. These results and the stoichiometry of the block co-polymer suggest that the soft domain rich in EO repeat units possibly orients to the PU crosslinks as previously described, and can be easily modulated chemically as desired. In details of EO-rich domain, in temperature regions II and III, the $\Delta\varepsilon_i$ of PU-AF slightly increases with respect to pristine PU in terms of $\alpha_{sEO,}$ while it is more or less of the same order of magnitude for α_{fEO}. These considerations suggest that two types of EO-rich domains are distinguished on the basis of the types of interactions existing between urethane moieties and soft EO-rich polymer blocks. The negligible change of $\Delta\varepsilon_{fEO}$ reflects the presence of ion-depleted EO-rich domain which is less affected by fixation of [Glyco]⁻ onto urethane moieties and presence of free [DEME]⁺. In the case of $\Delta\varepsilon_{sEO}$, the value increases upon fixation of [DEME][Glyco] to the PUs. This indicates that the strength of

inter-chain interactions in EO-rich domains with ions is higher compared to pristine PUs and this fact agrees with the low ε' at 1 Hz of PU-AF (see Fig. 4). On the contrary, in PU-CF and PU-IL, no peak associated to $\Delta\varepsilon_{sEO}$ mode is detected. This is easily explained if we consider that a high concentration of [Tf₂N]⁻ is present in these materials with respect to pristine PU, which interacts with the traces of both Na⁺ and K⁺ cations.[16] As a result of the interaction, [M(Tf₂N)₂]⁻ complexes are formed. Further confirmation of this information is obtained by comparing the values of E_a for conduction with those of the dielectric relaxations (see Fig. 8). Both E_a for conductivity and relaxation is respectively calculated from Eq. 4 and Eq. 5. It is observed that the E_a for conduction: 1) in PU and PU-AF materials is similar to that of α_{sEO}; and 2) in PU-CF and PU-IL, where a high density of anions "free" to complex the traces of alkaline cations which are present in soft EO-rich domains, is similar to the values of α_{fEO} mode. Results concur to demonstrate that two types of the long-range charge transfer mechanisms characterize the conductivity of proposed materials. These conductivities are modulated by the segmental motions of EO-rich repeat units in soft polyether domain in accordance with the following mechanisms. The first mechanism is observed in PU and PU-AF and occurs owing to the long-range charge migration events in bulk materials, which are taken place when cation exchange processes occur between EO repeat units. The second migration mechanism, which is responsible of the long-range charge migration events occurring in the samples with "free" [Tf₂N]⁻ (PU-CF and PU-IL), consists of two crucial steps. In the first step, the traces of mobile cations, such as Na⁺ and K⁺, are extracted from soft EO-rich domains by complexation of the cations with the [Tf₂N]⁻. The second step consists of the cation exchange processes through [Tf₂N]⁻ with a weak Lewis basicity:

$$Tf_2N + [M(Tf_2N)_2]^- \rightarrow [M(Tf_2N)_2]^- + Tf_2N$$
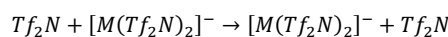
These events occur along percolation pathways originated between soft domains rich in EO repeat units. The long-range

and faster charge migration process in both PU-CF and PU-IL is significantly modulated by the fast segmental mode of in EO-rich domains. As a result, $[Tf_2N]^-$ are concluded to accelerate ion conduction and contribute to the antistatic effect. Taking into account both a higher antistatic effect and a lower possibility of bleeding out of ILs, cation fixation of $[Tf_2N]$ salts is the most suitable antistatic treatment of the PUs.

4. Conclusion

DC and BES measurements are carried out to study the mechanisms of current enhancement of the PUs after addition of ILs. In DC measurements, initial $I_c(t)$ are respectively found to be 0.0075 and 3.6 nA cm^{-2} for pristine PU and PU-CF (cation-fixed system). The latter number is high enough to enhance antistatic effect (indeed, their resistivity is lower than 10^{10} ohm cm^{-2}). In the case of the PU-CF, the superposition principle is not commutative, and $I_c(t-t_1) - I_\infty(t_1)$ is found to be ten times higher if compared to $-I_d(t)$. This suggests that the conductivity is enhanced not only by the relaxation of materials but also through electrode polarization. The stoichiometric discussion demonstrates that there exist enough ions which contribute to initial $I_c(t)$; however, the number of ions in PU-CF is insufficient to keep $I_\infty(t)$. BES measurements are carried out to discuss the details of the relaxation phenomena. Pristine PU and PU-AF are characterized by four dielectric relaxation processes. Two relaxations are associated with the domains rich in PO; *i.e.*, α_{fPO} and α_{sPO}. The other two relaxations show the following features. The one at the higher frequency is originated in ion-depleted EO-rich domains (α_{fEO}); the other, observed at lower frequencies, arises from the α_{sEO} relaxation of EO-rich domains coordinating with traces of alkaline and alkaline-earth ions. In this case, the conductivity is enhanced by cation exchange reactions in EO/ion complex. On the other hand, the PUs containing "free" anions such as PU-CF and PU-IL show two relaxations for PO-rich domains but show only α_{fEO} for EO-rich domains. The slow relaxation of the EO coordinating ions is absent in PU-CF and PU-IL due to the extraction of the metal ions by $[Tf_2N]^-$ ligands. The higher conductivity of the PU films comprising "free" $[Tf_2N]^-$ in comparison with that of pristine PU and PU-AF suggests that the migration of free ions is crucial to achieve an antistatic effect. From these results, "free" $[Tf_2N]^-$ are concluded to be a trigger for both long-range ion conduction and antistatic effect. Furthermore, PU-CF is not expected to bleed out of ionic species; accordingly, it should show a longer shelf life than PU-IL. Taken all together, the conductivity and antistatic properties arising from $[Tf_2N]^-$ and the long shelf life make the PU-CF the most promising system. Thus, the cation fixation of $[Tf_2N]$ salts is the most suitable antistatic treatment of the PUs.

Acknowledgements

References

1 (a) M. Armand, F. Endres, D. R. MacFarlane, H. Ohno, B. Scrosati, *Nature Materials,* 2009, **8**, 621; (b) V. Di Noto, S. Lavina, G. A. Giffin, E. Negro, B. Scrosati, *Electrochim. Acta,* 2011, **57**, 4.

2 (a) A. Tsurumaki, J. Kagimoto, H. Ohno, *Polym. Adv. Technol.*, 2011, **22**, 1223; (b) J. Shin, W. A. Henderson, S. Passerini, *Electrochem. Commun.*, 2003, **5**, 1016.

3 (a) D. K. Chattopadhyay, K. V. S. N. Raju, *Prog. Polym. Sci.*, 2007, **32**, 352; (b) Y. Jung, J. Kim, T. Hayashi, Y. Kim, M. Endo, M. Terrones, M. S. Dresselhaus, *Macromol. Rapid Commun.*, 2012, **33**, 628.

4 (a) S. Oprea, *J. Mater. Sci.*, 2011, **46**, 2251; (b) F. Xie, F. Guo, *Adv. Mat. Res.*, 2013, **704**, 289; (c) M. F. Sonnenschein, B. L. Wendt, *Polymer*, 2013, **54**, 2511; (d) M. Patri, S. K. Rath, U. G. Suryavansi, *J. Appl. Polym. Sci.*, 2006, **99**, 884.

5 A. Zheng, X. Xu, H. Xiao, N. Li, Y. Guan, S. Li, *Appl. Surf. Sci.*, 2012, **258**, 8861.

6 (a) D. Chen, J. Yang, G. Chen, *Compos. Part A: Appl. Sci. Manuf.*, 2010, **41**, 1636; (b) M. T. Byrne, Y. K. Gun'ko, *Adv. Mater.*, 2010, **22**, 1672; (c) M. Sangermano, S. Pegel, P. Pötschke, B. Voit, *Macromol. Rapid Commun.,* 2008, **29**, 396.

7 T. Iwata, A. Tsurumaki, S. Tajima, H. Ohno, *Macromol. Mat. Eng.*, 2014, **299**, 794.

8 A. Tsurumaki, S. Tajima, T. Iwata, B. Scrosati, H. Ohno, *Electrochim. Acta*, 2015, **175**, 13.

9 T. Iwata, A. Tsurumaki, S. Tajima, H. Ohno, *Polymer,* 2014, **55**, 2501.

10 A. Schönhals, *Acta Polymerica*, 1991, **42**, 149.

11 (a) V. D. Shtraus, *Polymer Mechanics*, 1976, **12**, 457; (b) M. E. Baird, *Rev. Mod. Phys.*, 1968, **40**, 219.

12 F. Bertasi, K. Vezzù, G. A. Giffin, T. Nosach, P. Sideris, S. G. Greenbaum, M. Vittadello, V. Di Noto, *Int. J. Hydrogen Energy*, 2014, **39**, 2884.

13 (a) V. Di Noto, M. Furlani, S. Lavina, *Polym. Adv. Technol.*, 1996, **7**, 759; (b) V. Di Noto, M. Vittadello, K. Yoshida, S. Lavina, E. Negro, T. Furukawa, *Electrochim. Acta*, 2011, **57**, 192; (c) M. Piccolo, G. A. Giffin, K. Vezzù, F. Bertasi, P. Alotto, M. Guarnieri, V. Di Noto, *ChemSusChem*, 2013, **6**, 2157.

14 (a) V. Di Noto, M. Vittadello, S. G. Greenbaum, S. Suarez, K. Kano, T. Furukawa, *J. Phys. Chem. B*, 2004, **108**, 18832; (b) V. Di Noto, G. A. Giffin, K. Vezzù, M. Piga, S. Lavina, *Solid State Proton Conductors: Properties and Applications in Fuel Cells,* John Wiley & Sons, **2012**, Chapter 5, 109-183.

15 V. Di Noto, *J. Phys. Chem. B*, 2002, **106**, 11139.

16 (a) J. C. Lassègues, J. Grondin, C. Aupetit, P. Johansson, *J. Phys. Chem. A,* 2009, **113**, 305; (b) G. A. Giffin, A. Moretti, S. Jeong, S. Passerini, *J. Phys. Chem. C*, 2014, **118**, 9966.

	Anion-fixed	Cation-fixed	IL-added
Antistatic	✗	✓	✓
Durability	✗	✓	✗